Experimental Investigation of Time Reversal Precoding for Space-Time Focusing in Wireless Communications

H. El-Sallabi, P. Kyritsi, A. Paulraj and G. Papanicolaou

Author contact information

Hassan El-Sallabi, hsallabi@polariswireless.com

Persefoni Kyritsi, persa@es.aau.dk (corresponding author)

Arogyaswami Paulraj, apaulraj@stanford.edu

George Papanicolaou, papanico@math.stanford.edu

Abstract

This work presents the results of indoor wideband measurements investigating the space-time properties of wireless signal transmission with online time reversal precoding. The measurements were conducted using a new time-reversal wideband MIMO channel sounder operating at 2.45 GHz with a bandwidth of 240 MHz. Both line of sight and non line of sight propagation conditions were investigated. Spatial focusing and temporal compression can be seen clearly with time reversal precoding, which may be useful for future wireless systems applications. Channel hardening due to time reversal is also observed under both line and non line of sight conditions.

Experimental Investigation on Time Reversal Precoding for Space-Time Focusing in Wireless Communications

H. El-Sallabi, P. Kyritsi, A. Paulraj and G. Papanicolaou

Abstract

This work presents the results of indoor wideband measurements investigating the space-time properties of wireless signal transmission with online time reversal precoding. The measurements were conducted using a new time-reversal wideband MIMO channel sounder operating at 2.45 GHz with a bandwidth of 240 MHz. Both line of sight and non line of sight propagation conditions were investigated. Spatial focusing and temporal compression can be seen clearly with time reversal precoding, which may be useful for future wireless systems applications. Channel hardening due to time reversal is also observed under both line and non line of sight conditions.

I. Introduction

Future wireless systems are expected to provide high data rate services to users. To achieve this the system bandwidth needs to be wider than that of current systems. Larger bandwidths will result in higher resolution of multipath components than what current systems can resolve, and will influence receiver design. Receiver designs based on equalization techniques are increasingly complex for channels with large multipath-induced root mean square (rms) delay spread and more difficult for diffuse channels, which have multipath components almost all over the channel delay window, that is, they have a very large number of significant channel taps. For example a maximum likelihood receiver has complexity that grows exponentially with the length of the channel. One

widely known approach for addressing this issue is the use of orthogonal frequency division multiplexing (OFDM) techniques to convert the wideband channel into a group of narrowband channels, for which the receiver design is simpler. Another possible approach is to use time reversal (TR), which is a technique that compresses the wideband energy temporally and focuses it spatially. TR requires channel state information (CSI) at the transmitter in order to precode the signal before transmission.

TR techniques have been studied extensively in acoustics [1-3], where experiments demonstrated that underwater TR communications is feasible. More recently, TR has been considered in wireless applications [4-8]. TR techniques transfer some the complexity of the communications system to the transmitter side. The TR system precodes the transmitted signal by a matched filter at the transmitter side (the matched filter is the time reversed and phase conjugated version of the channel impulse response). Wideband TR systems have three main properties: temporal compression, spatial focusing and channel hardening. Temporal compression implies that the delay window over which the effective channel impulse response is significant is reduced and the major part of the energy is aggregated near the main peak. Spatial focusing implies that the signal energy is focused at the intended receiver antenna (or user in the multi-user case) and is low at the locations of other users. Spatial focusing may be utilized in lowering co-channel interference in multi-cell/user systems, which leads to more efficient use of the bandwidth. Moreover, spatial focusing suggests that the system may have low probability of intercept features, that is, a nearby receiver of similar complexity would be unable to successfully decode the signal. Experimental demonstration of temporal compression of wideband signals over radio channels is presented in [9,10], and spatial focusing is

discussed in [11]. Channel hardening implies that there is an increased stability in the channel statistics after the application of TR, and therefore may reduce fading.

This work investigates experimentally the spatial and temporal focusing properties of time reversed signals, as well as the resulting channel hardening. The measurements were conducted in an indoor environment using a TR wideband MIMO channel sounder. Section II presents the formulation of the problem and introduces measures for temporal and spatial focusing. The experimental system setup is described in Section III. Measurement results are discussed in Section IV. The paper ends with some conclusions and a discussion of future work.

II. Problem formulation

Consider a wireless system with M transmit antennas and P receive antennas, and let $h_{p,m}(t;\tau, r_m \to r_p)$ be the channel impulse response (CIR) measured at time t from a transmitter at location r_p to a receiver at location r_m, with τ denoting the delay of the multipath components of the measured CIR.

In TR precoding, the transmitter m applies a filter $g_m(t)$, the impulse response of which is the time-reversed complex conjugate of the CIR to the intended receiver at location r_p, i.e.,

$$g_m(t;\tau) = K \cdot h^*_{p.m}(t;-\tau, r_m \to r_p). \tag{1}$$

Here K is a power normalization factor and * denotes the complex conjugate. The received signal $y_{p,m}(t)$ can be written as

$$y_{p,m}(t) = h_{p,m}(t;\tau, r_m \to r_p) \otimes g_m(t,\tau) \otimes x(t) + n(t) \tag{2}$$

where x(t) is the transmitted data, $n(t)$ is the receiver noise, and $\otimes$ denotes the convolution operation. If the channel is unchanged during the channel estimation and TR transmission, the equivalent TR channel impulse response from transmit antenna m to receive antenna p including the precoding filter without scaling can be written as

$$h_{m,p}^{eq}\left(t;\tau,r_m \to r_p\right) = h_{m,p}\left(t;\tau,r_m \to r_p\right) \otimes h_{m,p}^{*}\left(t;-\tau,r_m \to r_p\right) \tag{3}$$

This is the autocorrelation function of the CIR $h_{p,m}\left(t;\tau,r_m \to r_p\right)$.

If we observe the equivalent CIR in the time domain, we notice that the energy is compressed at the center of equivalent impulse response and is zero (or very low power) elsewhere.

In the frequency domain, the TR channel transfer function can be written as

$$H_{m,p}^{eq}\left(t;f,r_m \to r_p\right) = H_{m,p}\left(t;f,r_m \to r_p\right) H_{m,p}^{*}\left(t;f,r_m \to r_p\right). \tag{4}$$

In order to measure spatial focusing, we study the CIR at a location r_l when the signal has been precoded for an intended receiver at location r_p. This can be written as

$$h_{m,l|p}^{eq}\left(t;\tau,r_m \to r_l \mid r_p\right) = h_{m,l}\left(t;\tau,r_m \to r_l\right) \otimes h_{m,p}^{*}\left(t;-\tau,r_m \to r_p\right). \tag{5}$$

We measure the spatial focusing at location r_l using $\kappa_{MAX}\left(r_l\right)$ or $\kappa_0\left(r_l\right)$. Here $\kappa_{MAX}\left(r_l\right)$ is the peak power of the equivalent CIR $h_{m,l|p}^{eq}\left(t;\tau,r_m \to r_l \mid r_p\right)$, and $\kappa_0\left(r_l\right)$ is the power at a location r_l when the equivalent channel impulse response on the target achieves its maximum value, that is, at τ_0 where τ_0 is the delay of the peak of the equivalent CIR at the intended receiver:

$$\kappa_{MAX}\left(r_l\right) = \max_{\tau}\left|h_{m,l|p}^{eq}\left(t;\tau,r_m \to r_l \mid r_p\right)\right|^2, \quad \kappa_0\left(r_l\right) = \left|h_{m,l|p}^{eq}\left(t;\tau_0,r_m \to r_l \mid r_p\right)\right|^2. \tag{6}$$

We expect a reduction in $\kappa_{MAX}\left(r_l\right)$ and $\kappa_0\left(r_l\right)$ as the distance between the observation point r_l and the intended receiver location r_p increases.

III. Experimental setup

A. Measurement equipment

The measurement system is a new time-reversal wideband multiple input multiple output (MIMO) channel sounder that is based on the existing RUSK MIMO wideband channel sounder [12], the capabilities of which were extended to handle TR transmission based on designs by Stanford University and Medav [13].

The system operates with bandwidth up to 240 MHz centered at 2.45 GHz. It can handle up to 8 transmitter elements and up to 8 receiver elements. The antennas are connected to their terminals through RF switches that are capable of handling the transmit power. The transmitter sends signals in a time multiplexing scheme from the different transmit antennas, which are consequently received and recorded in a time multiplexed fashion by the receive antennas. The RF switches at both terminals are synchronized before conducting the measurements.

B. Measurement equipment operation

The TR-MIMO channel sounder works in two modes: the sounding mode and the TR mode. In the sounding mode, the sounder measures the channel transfer functions for a certain number of blocks of MIMO snapshots. The measurement is performed using multitone signals of equal amplitude but with carefully designed phases to reduce the crest factor. After the receiver has captured a prescribed number of blocks and snapshots, it sends a control signal to the transmitter to switch to TR mode. In TR operation, CSI is required at the transmitter side. The estimated channels can be fed back to the transmitter as CSI through various possible feedback channels, e.g., wireless LAN, Ethernet or optical fiber, under the constraint that the feedback channel should be fast enough to guarantee channel invariance between the channel estimation and the data transmission.

For this set of measurements, an optical fiber was used to feed back the CSI. Finally, during TR transmission the back fed channels are used for the precoding filter, which processes the message to be transmitted before transmitting it into the channel. The received signal is the TR signal.

C. Measurement setup

A 2x2 MIMO indoor measurement campaign was conducted in the Packard Electrical Engineering building at Stanford University. The measurements were conducted during off-peak hours to avoid high channel variability. The locations of both the transmitter and the intended receiver were fixed. The transmit antenna was placed at a height of 6 ft and the receive antenna at a height of about 4 ft. For our experiments, the transmit antennas were sectorized directional antennas and the receiver antennas were omni-directional. All antenna elements were vertically polarized.

The measurement campaign included both line of sight (LOS) and non line of sight (NLOS) propagation conditions. The LOS experiments were conducted in a heavily equipped laboratory room. The distance between transmitter and receiver was about 10 ft, and the transmitted sequence length was 0.8 μs. The transmitted sequence length is selected so that it exceeds the maximum delay of the impulse response in the environment in order to avoid temporal aliasing. The NLOS measurements were conducted in the main hall of the building and the distance between the transmitter and the receiver was about 120 ft. The transmitted sequence length was 1.6 μs.

For the spatial focusing studies, one receive antenna was fixed at a corner of a rectangular grid and was considered as the intended receiver. The other antenna was shifted in the virtual grid with a spacing of about $\lambda/2$ (=2.41in) of the center frequency. The

measurement grid was about 2ft × 1ft. The transfer function between one transmit antenna and the target receive antenna was used for prefiltering, and the equivalent channel transfer function was measured at the different observation points on the synthetic rectangular array.

The measurement data were calibrated so that the effect of both the transmitter and the receiver equipment and the effect of the cabling were removed, but the effect of the transmit antenna directivity was not removed. The measured channel transfer functions and TR channels were stored on a local hard disk for further processing.

IV. Measurement results

A. Temporal focusing

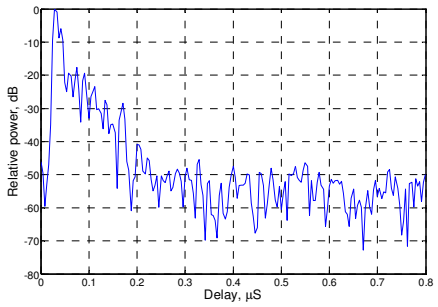

(a) LOS original CIR

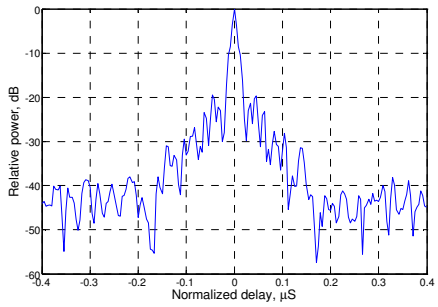

(b) LOS equivalent CIR with TR

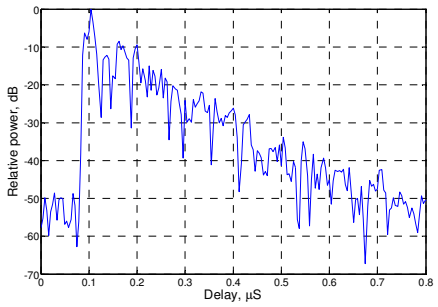

(c) NLOS original CIR

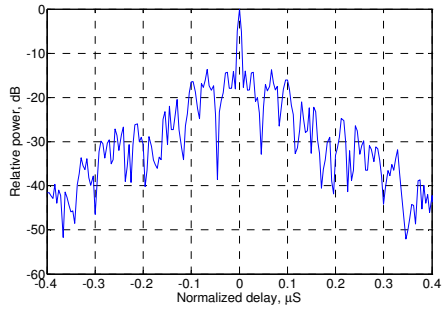

(d) NLOS equivalent CIR with TR

Figure 1: CIR with and without TR in LOS and NLOS situations

Fig. 1 shows samples of the original and the equivalent measured power delay profile at the intended receiver under both LOS and NLOS propagation conditions. The time domain functions were obtained by inverse Fourier transform of the frequency-domain measurements. The responses have been normalized to their maximum value. Clearly the original CIR in the NLOS case shows larger delay spread. The equivalent CIRs after TR show that most of the energy is concentrated around a narrow peak, and the temporal sidelobes are suppressed by about 10 dB. This indicates that there is temporal compression, which is more obvious in the NLOS case than the LOS case.

B. Spatial focusing

Fig. 2 shows a 2D plot of the spatially focused power measured as $\frac{\kappa_0(r_l)}{\kappa_0(r_p)}$ in (a) and (c), and $\frac{\kappa_{MAX}(r_l)}{\kappa_{MAX}(r_p)}$ in (b) and (d), under both LOS and NLOS conditions, averaged over the recorded snapshots. In all the figures the received power is maximum at the location of the intended receiver. This demonstrates clearly the spatial focusing properties of TR precoding. In LOS situations, $\frac{\kappa_{MAX}(r_l)}{\kappa_{MAX}(r_p)}$ and $\frac{\kappa_0(r_l)}{\kappa_0(r_p)}$ are as low as 11 dB and 15 dB below the peak measurement on the grid. The mean of the reduction over all measured points in the spatial grid is about 6 dB. In NLOS situations, $\frac{\kappa_{MAX}(r_l)}{\kappa_{MAX}(r_p)}$ and $\frac{\kappa_0(r_l)}{\kappa_0(r_p)}$ are as low as about 13 dB and 28 dB below the peak over the grid, respectively, and the average peak power reduction of $\frac{\kappa_{MAX}(r_l)}{\kappa_{MAX}(r_p)}$ and $\frac{\kappa_0(r_l)}{\kappa_0(r_p)}$ over the grid is 8 dB and 14 dB at locations r_l, where $r_l \neq r_p$. Spatial focusing measured by $\frac{\kappa_0(r_l)}{\kappa_0(r_p)}$ is stronger for NLOS as expected.

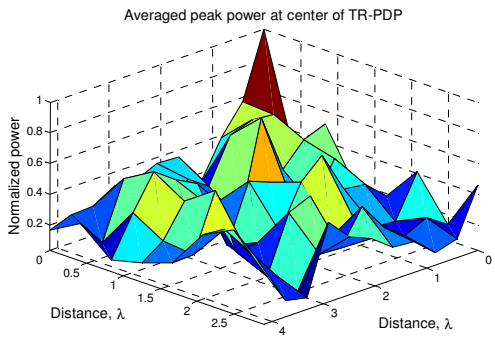

(a) LOS situation, $\frac{\kappa_0(r_l)}{\kappa_0(r_p)}$ (linear scale).

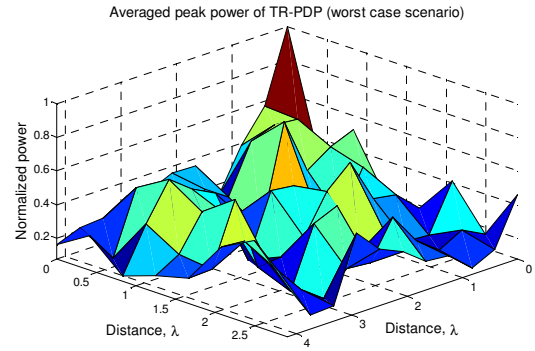

(b) LOS situation, $\frac{\kappa_{MAX}(r_l)}{\kappa_{MAX}(r_p)}$ (linear scale).

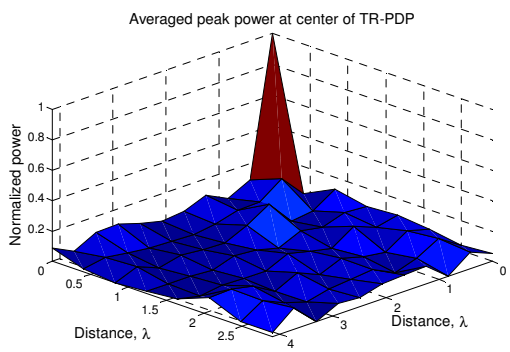

(c) NLOS situation, $\frac{\kappa_0(r_l)}{\kappa_0(r_p)}$ (linear scale).

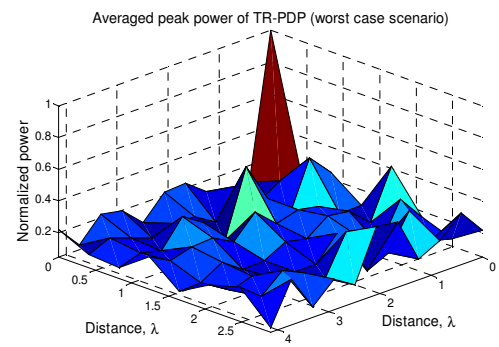

(d) NLOS situation, $\frac{\kappa_{MAX}(r_l)}{\kappa_{MAX}(r_p)}$ (linear scale).

Figure 2: Spatial focusing

C. Channel hardening

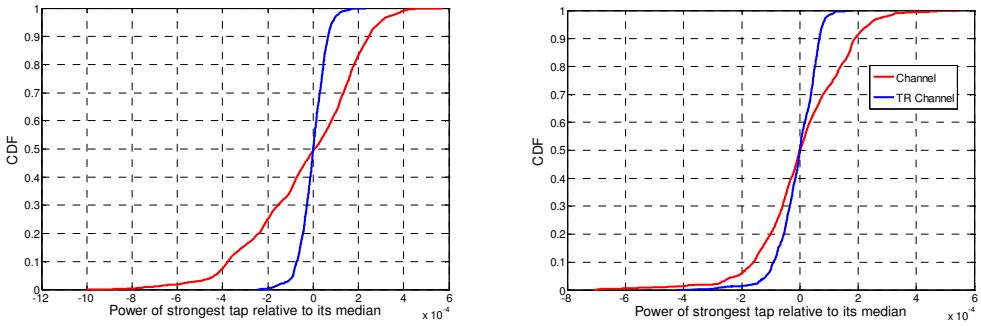

(a) Channel hardening in LOS (b) Channel hardening in NLOS

Figure 3: CDF of the maxima of the CIR.

Fig. 3 shows the cumulative density function (cdf) of the maximum of the CIR with and without TR in both LOS and NLOS situations. The plots have been normalized to their respective median values. There are several possible reasons for the spread of the maxima of the CIR in the case without TR. First, it can be due to measurement noise, which in our case noise was negligible. Second, it can be due to channel variability over one block (where one block corresponds to the set of measurements taken for a single combination of intended receiver non-intended receiver locations). Although not shown here, the cdf over one block shows that this variability is negligible. Third, it can be due to channel variability over many blocks. The cdf shown here is over all measurements of intended receiver and non-intended user locations. Clearly, even if the target is at the same location, the other antenna acts as scatterer in the environment and changes the CIR. Therefore, the spread in the cdf is observable. TR reduces variations due to this effect.

V. Conclusion

We have presented an experimental investigation of the spatio-temporal focusing and channel hardening properties of time reversal wireless in an indoor environment. Both LOS and NLOS propagation conditions have been investigated for fixed indoor channels. Future work will consider spatio-temporal focusing and channel hardening for mobile channels.

Acknowledgement.

This work was supported by ONR grant number N00014-02-1-0088.

References:

[1] M. Fink, D. Cassereau, A. Derode, C. Prada, P. Roux, M. Tanter, J. -L. Thomas, and F. Wu, "Time-reversed acoustics," in *Rep. Prog. Phys.* 63, pp**.** 1933–1995, 2000.

[2] A. Derode, P. Roux, and M. Fink, "Robust acoustic time reversal with high-order multiple scattering," *Phys. Rev. Letters*, vol. 75, pp. 4206–4209, 1995.

[3] D. Rouseff, D. R. Jackson, W. L. J. Fox, C. D. Jones, J. A. Ritcey, and D. R. Dowling, "Underwater Acoustic Communication by Passive-Phase Conjugation: Theory and Experimental Results," in *IEEE J. Ocean. Eng.* 26, pp. 821-831 (2001).

[4] C. Oestges, A.D. Kim, G. Papanicolaou, and A.J. Paulraj, "Characterization of space-time focusing in time reversed random fields," in *IEEE Trans. Antennas and Prop*, vol. 53, pp. 283-293, 2005.

[5] T. Strohmer, M. Emami, J. Hansen, G. Papanicolaou, and A. Paulraj, "Application of Time-Reversal with MMSE Equalizer to UWB Communications," in *Proc. IEEE GLOBECOM '04*, vol. 5, pp. 3123 – 3127.

[6] P. Kyritsi, P. Stoica, and G. Papanicolaou, "Time reversal and zero-forcing for WLAN applications," in *Proc. WPMC* 2005.

[7] H.T. Nguyen, J. B. Andersen, and G.F. Pedersen, "The potential use of time reversal techniques in multiple element antenna systems," in *IEEE Communications Letters*, vol. 9, no 1, pp. 40- 42, Jan. 2005.

[8] H.T. Nguyen, J.B. Andersen, G.F. Pedersen, P. Kyritsi, and P. Eggers, "Time Reversal in Wireless Communications a Measurement Based Investigation," in *IEEE Trans. in Wireless Comm.*, vol. 5, no. 8, pp.2242-2252, August 2006.

[9] G. Lerosey, J. de Rosny, A. Tourin, A. Derode, G. Montaldo, and M. Fink, "Time Reversal of electromagnetic waves," in *Physical Review Letters*, no 92, 2004.

[10] P. Kyritsi, G. Papanicolaou, P. Eggers, and A. Opera, "MISO time reversal and delay spread compression for FWA channels at 5 GHz," in *Antennas and Wireless Propagation Letters,* vol. 3, pp. 96-99, 2004.

[11] B.E. Henty, and D.D. Stancil, "Multipath-enabled super-resolution for RF and microwave communications using phase-conjugate arrays," in *Physical Review Letters*, no 93, December 2004.

[12] www.channelsounder.de

[13] www.medav.com